Published online November 27, 2005

Nucleic Acids Research, 2005, Vol. 33, No. 20 ***e176***
doi:10.1093/nar/gni180

Footprinting of mammalian promoters: use of a CpG DNA methyltransferase revealing nucleosome positions at a single molecule level

Mehrnaz Fatemi, Martha M. Pao, Shinwu Jeong, Einav Nili Gal-Yam, Gerda Egger, Daniel J. Weisenberger and Peter A. Jones*

Department of Urology, Biochemistry and Molecular Biology, USC/Norris Comprehensive Cancer Center, Keck School of Medicine, University of Southern California, Los Angeles, CA 90089-9181, USA

Received June 7, 2005; Revised September 9, 2005; Accepted October 31, 2005

ABSTRACT

Promoters are molecular 'modules', which are controlled as individual entities yet are often analyzed by nuclease digestion methodologies which, *a priori*, destroy this modularity. About 40% of mammalian genes contain CpG islands in their promoters and exonic regions, which are normally unmethylated. We developed a footprinting strategy to map the chromatin structure at unmethylated CpG islands by treatment of isolated nuclei with the CpG-specific DNA methyltransferase SssI (M.SssI), followed by genomic bisulfite sequencing of individual progeny DNA molecules. This gave single molecule resolution over the promoter region and allowed for the physical linkage between binding sites on individual promoter molecules to be maintained. Comparison of the *p16* promoters in two human cell lines, J82 and LD419, expressing the *p16* gene at 25-fold different levels showed that the two cell lines contain remarkably different, heterogeneously positioned nucleosomes over the promoter region, which were not distinguishable by standard methods using nucleases. Our high resolution approach gives a 'digitized' visualization of each promoter providing information regarding nucleosome occupancy and may be utilized to define transcription factor binding and chromatin remodeling.

INTRODUCTION

Each promoter molecule in a cell can be considered a module which is controlled individually. Increased levels of overall gene expression can be achieved by increasing the number of promoters functioning or the frequency by which they initiate transcription. Although there is this fundamental modularity to promoter function, most approaches to chromatin structure analysis rely on methods such as nuclease digestion which give average results of all the molecules of a given promoter in a cell population and destroy the physical linkages between binding sites obscuring this individuality. (1,2).

Nucleosomal positioning, [reviewed in (3–8)] and the modification status of the histone tails (9,10), play central roles in controlling transcriptional initiation. Transcriptional co-activator complexes interact with nucleosomes (11) to induce nucleosomal rearrangements. Nucleosomes often have to unfold completely (12) or be disassembled (13) at the transcription start site, to allow for transcriptional initiation (14,15). Most studies focus on the extreme cases of the complete absence or presence of transcription, especially in yeast (16,17). In this paper, we examined nucleosomal arrangements in the *p16* promoter in human cell lines, J82 and LD419, which express the *p16* gene at 25-fold different levels.

We modified a previously described footprinting method (18), which now allows us to analyze how individual molecules are packaged into chromatin. We treated naked DNA, nucleosomes reconstituted *in vitro*, or nuclei from two cell lines expressing different levels of *p16* with an excess of the robust cytosine-C5 CpG-specific DNA methyltransferase SssI (M.SssI). Although this enzyme methylates all CpG sites in purified DNA, it cannot methylate the same sites when they are assembled into nucleosomes or are associated with tight-binding factors (18,19). By cloning and sequencing DNA molecules following bisulfite treatment, we discerned patches of accessible and inaccessible sites on individual DNA molecules, which reflect packaging of, or protein binding to, each promoter molecule for a given gene (Figure 1). This differs from conventional footprinting techniques relying on nuclease digestion and primer extension (4) in that the footprints are physically linked on individual DNA molecules showing potential simultaneous occupancy of factors controlling transcription.

*To whom correspondence should be addressed. Tel: +1 323 865 0816; Fax: +1 323 865 0102; Email: jones_p@ccnt.hsc.usc.edu

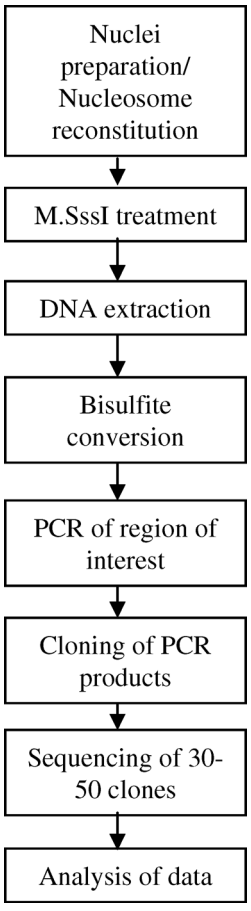

Figure 1. A flow diagram depicting the M.SssI footprinting method.

Our ability to assess nucleosomal positioning on individual DNA molecules reveals a remarkably heterogeneous pattern of nucleosome distribution on the *p16* promoter. Since many constitutive and tissue-specific promoters contain unmethylated CpG-island promoters, this approach, alone, or combined with current chromatin-studying methodologies, will provide a useful tool to dissect chromatin structures and changes at a single molecule level.

MATERIALS AND METHODS

Cell culture

The two cell lines, the normal fibroblasts LD419 and bladder cancer cells J82 were cultured and maintained as described previously (20).

Quantitative real-time PCR

Total RNA was extracted from the cultured LD419 and J82 cells by using RNeasy Kit (Qiagen) following manufacturer's protocols; reverse transcription and the quantification of mRNA levels was carried out by real-time PCR as described previously (21).

Rapid amplification of cDNA ends (5′-RACE)

Total RNA was extracted as described above and 5′ ends of mRNA were detected using the RLM-RACE Kit (Ambion)

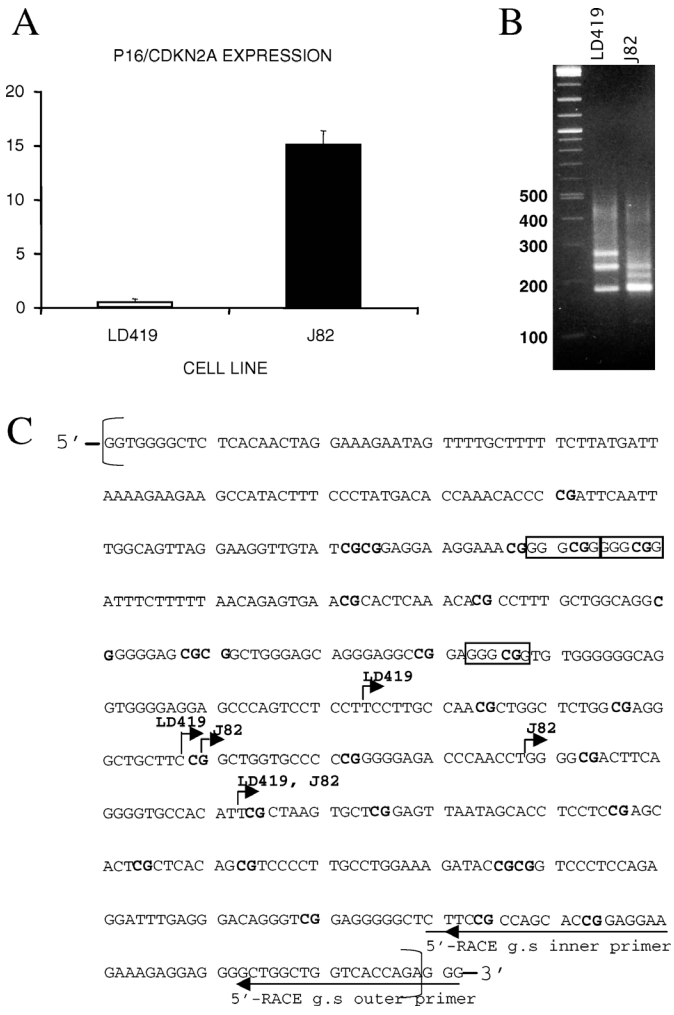

Figure 2. Analysis of *p16* gene expression and detection of TISs. (**A**) Relative expression levels of *p16* mRNA in LD419 and J82 cells (normalized to GAPDH) measured by quantitative real-time RT–PCR. The levels of mRNA expression in J82 cells are 25-fold higher than in LD419 cells. (**B**) The inner 5′-RACE PCR products of LD419 and J82 cell, analyzed on a 3% agarose gel. The three main PCR products of each cell line indicate the three TISs, whose 5′ ends were analyzed by DNA sequencing. Two of them were shared and one was unique to each cell type. (**C**) Sequence region of the *p16* promoter (529 bp) shown in square bracket, with 28 CpG sites, and location of GC boxes (shown as boxes). The 5′ ends of mRNA detected by 5′-RACE in the two cell lines (shown as bent arrow) and the primer sequences designed for outer and inner 5′-RACE PCR are indicated.

according to the manufacturer's protocols. The inner 5′ RLM-RACE PCR products were cut from a 3% agarose gel, purified using the Gel Extraction Kit (Qiagen) and sequenced with a inner gene-specific primer. The primer sequences are shown in Figure 2C.

Nuclei extraction

All procedures for nuclei isolation were performed at 4°C. Actively growing cells (10^8) were trypsinized and washed twice with cold phosphate-buffered saline. Cells were resuspended in 9 ml RSB buffer (10 mM Tris–HCl, pH 7.4, 10 mM NaCl and 3 mM $MgCl_2$) and kept on ice for 10 min. Following this incubation, 1 ml of 10% NP-40 detergent was added and

cells homogenized with 10–15 strokes of the tight pestle of a Dounce homogenizer. Nuclei were washed twice with RSB buffer to eliminate the detergent, followed by one wash with M.SssI buffer (10 mM Tris–HCl, pH 7.9, 50 mM NaCl, 10 mM $MgCl_2$, 1 mM DTT and 0.3 M sucrose). NaCl (0.4 M) was used to remove most non-histone-bound proteins from chromatin (22). Nuclei were washed once with RSB buffer and once with medium salt buffer (20 mM Tris–HCl, pH 7.4, 0.4 M NaCl, 1 mM EDTA and 5% Glycerol) followed by one wash with M.SssI buffer. Nuclei or salt-washed nuclei were resuspended in 1× M.SssI buffer to a concentration of 10^7 nuclei/ml. The quality of the salt-washed nuclei was tested by SDS–PAGE.

Nucleosome reconstitution

Core histone octamers were purified from chicken erythrocyte cells as described previously (23). Supercoiled plasmid DNA pSVO-CAT, containing an 870 bp DNA fragment of the *p16* promoter region (24), was purified using Wizard Plus Midipreps DNA Purification System (Promega). Reconstitutions were carried out by the salt dialysis method at 4°C as described previously (25). Core histone octamers were mixed with supercoiled plasmid DNA at equivalent amounts.

M.SssI treatments

Extracted nuclei or reconstituted nucleosomes were treated with M.SssI immediately after preparation for 15 min at 37°C. The methylation reactions were carried out in 1× M.SssI buffer with 160 μM SAM (supplied with M.SssI by New England Biolabs). Nuclei from 10^6 cells (≈6 μg DNA) in a total reaction volume of 150 μl or 1.5 μg reconstituted nucleosomes in a total reaction volume of 50 μl were treated with 60 and 15 U M.SssI, respectively. The activity of M.SssI was also tested using 6 μg of purified genomic DNA or 1.5 μg of plasmid DNA, respectively, under the same conditions as described above. Reactions were stopped by the addition of an equal volume of stop solution (20 mM Tris–HCl, pH 7.9, 600 mM NaCl, 1% SDS, 10 mM EDTA and 400 μg/ml proteinase K). Samples were incubated at 55°C for 16 h and DNA was purified by phenol/chloroform extraction and ethanol precipitation.

Methylation analysis using bisulfite genomic sequencing

Bisulfite genomic sequencing was used to analyze the methylation patterns of individual DNA molecules. The *p16* promoter was PCR amplified using DNA that had undergone M.SssI treatment followed by sodium bisulfite conversion (26). PCR conditions and the primer sequences for the *p16* promoter have been previously described (27). PCR products were then cloned into the pCR2.1 vector provided by TOPO-TA Cloning Kit (Invitrogen) following the manufacturer's instructions. The positive screened colonies contained the unique sequence of one individual DNA molecule. The plasmid DNA from the selected positive colonies containing vectors with the *p16* promoter inserts was purified using the Qiagen plasmid Mini Kit. The purified plasmids were sequenced at the region of interest. Between 30 and 50 individual sequences were performed for each nuclear preparation. In order to exclude a sampling error we performed Ms-SNuPE analysis on six individual CpG sites within the *p16* region using the same PCR products which were later cloned. The methylation levels obtained by Ms-SNuPE were comparable with the total methylation of these sites for all sequenced molecules (data not shown). Sequencing was performed at the USC/Norris Microchemical Sequencing Core Facilities. A flow diagram of the method is depicted in Figure 1.

Indirect end labeling

Nuclei from the cultured LD419 and J82 cells were isolated as described above. Nuclei were resuspended in 1× MNase buffer (10 mM Tris–HCl, pH 8.0, 100 mM NaCl and 1 mM EDTA) after two washes with cold RSB buffer to a DNA concentration of ≈50 μg/ml. A total of 400 μl nuclei aliquots were used for MNase digestion in a total reaction volume of 450 μl containing 2 mM $CaCl_2$. Nuclei were digested with increasing concentrations of MNase (0, 0.25–28 U/ml) for 15 min at 37°C. Reactions were stopped by the addition of 50 μl of 10× stop solution (1% SDS, 100 mM EDTA). Freshly dissolved proteinase K was added to a concentration of 200 μg/ml and samples were incubated at 55°C for several hours or overnight. DNA was purified by phenol/chloroform extraction and ethanol precipitation. Qualities of MNase digestions were checked on a 1.5% agarose gel and the appropriate digestion products were selected for Southern hybridization. Partial MNase digested DNA was cut by DraI and subsequently fractioned on a 1.5% agarose gel with a molecular weight marker and then Southern blotted. The blot was hybridized with a 250 bp PCR amplified DraI-probe, which is located 896 bp apart and upstream of the most downstream transcription initiation site (TIS) of *p16/CDKN2A*. Labeling of the probe was performed with [α-^{32}P]dCTP using High Prime (Roche), and for hybridization the ExpressHyb Hybridization Solution (BD Biosciences) was used according to the manufacturer's instructions. The PCR primer sequences for the probe are sense: 5′-AAACTCACAACAACCCCTATAAAGC-3′ and antisense: 5′-TAGGCAGATAGGAAAATGGGG-3′. Visualization of the bands was achieved by exposure of the blot to Kodak BioMax MR film at −80°C for 7 days.

RESULTS

Expression and transcription initiation sites of the *p16* gene

We have previously defined and characterized the *p16/CDKN2A* promoter (24), which together with exon 1 of this gene is located in a CpG island that is unmethylated in both LD419 fibroblasts and J82 bladder cancer cells (28). Quantitative real-time PCR showed that the J82 bladder cancer cell line expressed ∼25 times more *p16* mRNA at the steady-state level than the normal fibroblasts (Figure 2A). Since both cell types have little or no cytosine methylation in the promoter region, the different levels of expression cannot be caused by DNA cytosine methylation. However, it might be due to altered states of chromatin structure which may cause, or be a consequence of, transcription factor recruitment to the promoter. In common with several CpG island promoters, RNase protection analysis has shown evidence of multiple *p16* TISs (29); however, the locations of these TISs were not identified precisely and the cell types used differed from our study. We applied 5′-RACE to identify the 5′ ends of *p16* mRNAs in

LD419 and J82 cell lines. Both cell lines showed three TISs, two of which were shared and one was unique to each cell type (Figure 2B and C). The results of the sequencing of the 5′-RACE-generated transcripts are shown in Figure 2C. The three 5′-RACE-generated mRNAs in the LD419 cell were of equal abundance; however, in J82 cells the shorter transcript (173 bp PCR product) appeared stronger than the other two mRNAs (Figure 2B).

Nucleosomal positioning on the *p16* promoter

The apparent 'positioning' of nucleosomes can be determined by nuclease digestion; however, this approach gives an average for all promoter molecules and does not directly show whether all promoters are organized in the same manner. To assess the average distribution of nucleosomes, we next treated nuclei isolated from both cell types with micrococcal nuclease (MNase) and analyzed the digestion products by Southern blotting (Figure 3). In LD419 cells at least three positioned nucleosomes were apparent over the promoter region (II, III and IV), of which the nucleosomal intervals were ~200 bp (II and III) and 180 bp (IV), consistent with an approximate 190 bp of bulk nucleosomal repeat length. Nucleosome I may also be positioned; however, its upstream boundary could not be defined as the naked DNA control also showed a hypersensitive site in this region. Interestingly, nucleosomes I and II encompassed the TISs and GC boxes. This might potentially restrict access of this region to RNA polymerase II and transcription factors and might contribute to the lower levels of expression in these cells relative to the J82 bladder cancer cells.

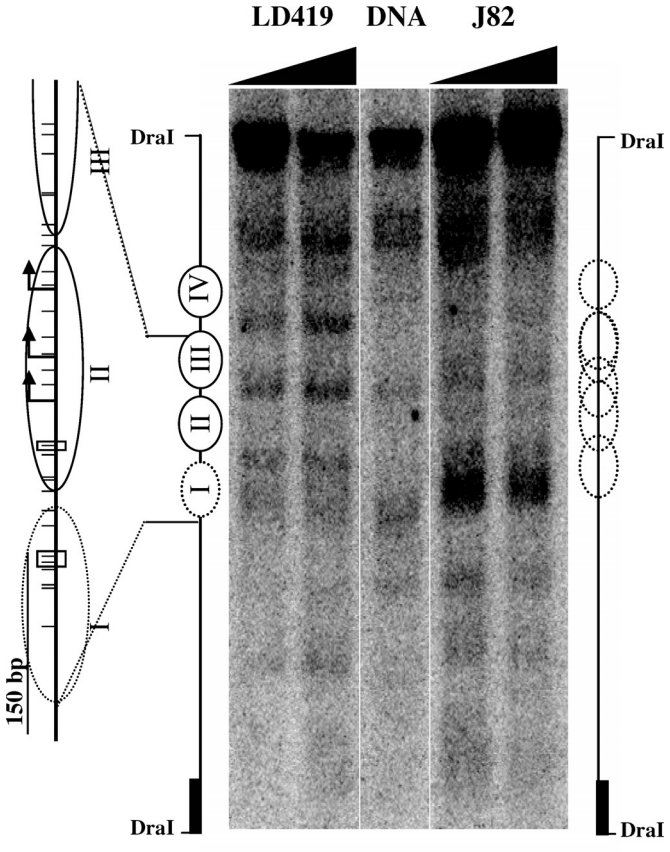

Figure 3. Nucleosome positions within the *p16* promoter region mapped by indirect end-labeling. Nuclei from the low *p16* expressing LD419 human fibroblasts, high *p16* expressing J82 bladder cancer cells and naked DNA were partially digested with MNase. The cutting sites were mapped from the DraI site shown in the figure. The location of the DraI-probe is indicated as a black box. Positioned nucleosomes are indicated as white ovals with solid lines, and random arrangement of nucleosomes by a dotted line. Bent arrows indicate transcription start sites within the *p16* promoter. The map of the *p16*/*CDKN2A* promoter is drawn to scale and indicates the sequenced regions containing 28 CpG sites (tick marks above the line), location of GC boxes (shown as boxes) and TISs of LD419 and J82 cell lines.

Uniformly positioned nucleosomes at the more active *p16* promoter in J82 cells were difficult to define by the MNase assay, possibly due to enhanced nucleosomal mobility (11,30). This suggests that the two cell lines may have quite different chromatin structures at this promoter. Furthermore, a distinct MNase hypersensitive region was detected in the region of nucleosome I, which was not detected in either the LD419 cells or the naked DNA control. This seems to be consistent with the observation that many promoter molecules in J82 cells were free of nucleosomes in this region in the M.SssI analysis (see below).

These results encouraged us to modify the method pioneered by Kladde and Simpson (18) for probing chromatin structure at a single molecule resolution.

M.SssI catalyzed methylation of the *p16* promoter CpG Island in purified DNA

We took advantage of previous studies which have shown that nucleosomes or DNA binding proteins can block methylation by the CpG-specific DNA methylase M.SssI (18,19). Unlike these earlier studies in which the bulk of the bisulfite treatment reaction products were sequenced, we cloned individual DNA molecules before sequencing to probe for the position of nucleosomes at single DNA molecule resolution.

Initially, we determined the kinetics of methylation of DNA purified from human sperm by M.SssI to establish a baseline upon which the accessibility of CpG sites in genomic DNA and chromatin could be compared. The level of methylation in untreated sperm DNA was negligible at the *p16* promoter (Figure 4). The enzyme modified 71% of the CpG sites at the *p16* promoter after 7 min and methylation levels reached near saturation after 15 min (data not shown). While there was some slight preference for methylation of individual CpG sites at the intermediate times of incubation, these did not differ much from each other at 15 min (data not shown). Analysis of the reaction products of chromatin fractions incubated with M.SssI might therefore provide a footprinting method, which would give single molecule resolution.

Methylation of *in vitro* reconstituted nucleosomes

Nucleosomes reconstituted on a cloned *p16* promoter were treated with M.SssI for 15 min and individual DNA molecules sequenced to define whether nucleosomal DNA was inaccessible to M.SssI at the *p16* promoter (Figure 5). As a control, naked supercoiled plasmid DNA was treated with M.SssI as well. Most cloned DNA molecules derived from reconstituted nucleosomes contained patches of CpG sites, which were inaccessible to the DNA methyltransferase; however, the naked

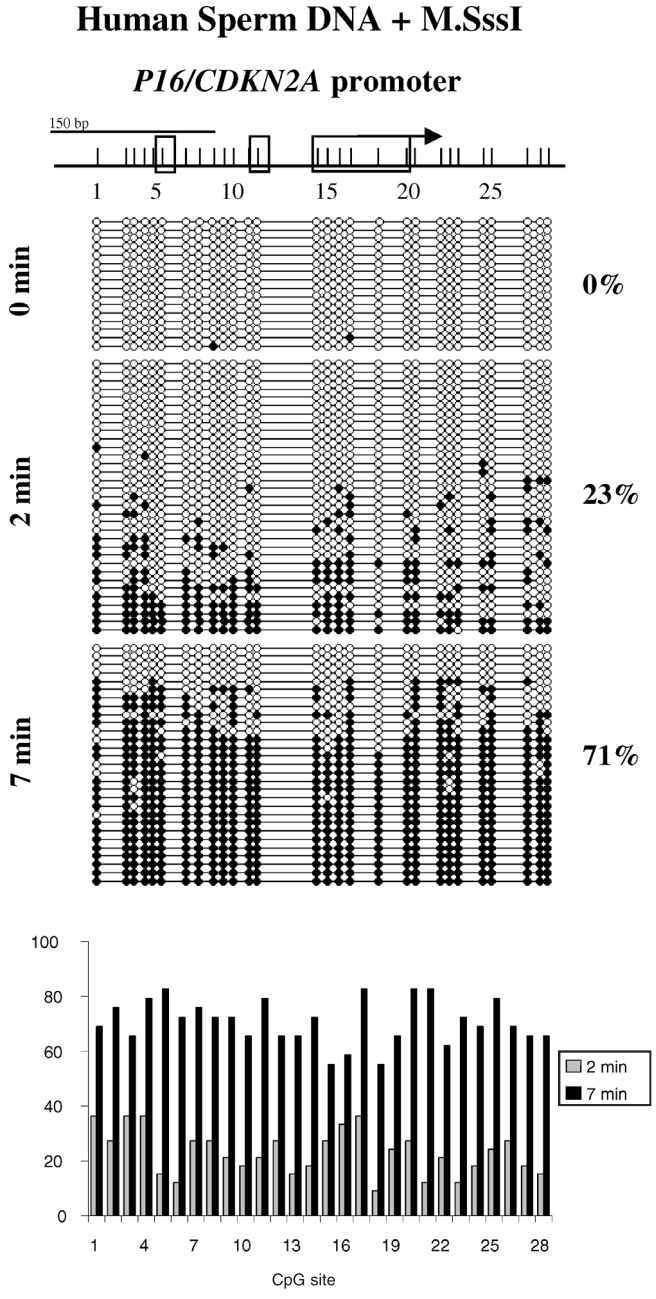

Figure 4. Kinetics of methylation of purified human sperm DNA by M.SssI at the *p16* promoter. Following bisulfite conversion and cloning of DNA, individual molecules were sequenced. Each horizontal line with a string of circles represents the methylation profile for one DNA molecule. White circles indicate unmethylated and black circles methylated CpG sites. The diagram on the top, drawn to scale represents the region analyzed and indicates the distribution density of CpG sites. The block with a bent arrow shows the region of transcription start sites detected by the 5′-RACE assay in LD419 and J82 cells. The location of GC boxes is indicated as small boxes. The overall level of methylation of all molecules at each time point is noted to the right of the molecules as a percentage. Bottom: the methylation status of individual CpG sites at the *p16* promoter region after 2 and 7 min incubation of purified DNA with M.SssI.

plasmid DNA was completely methylated (data not shown). Interestingly, the analysis of single promoter sequences showed a substantial number of inaccessible regions with overlapping positions. The presence of inaccessible patches

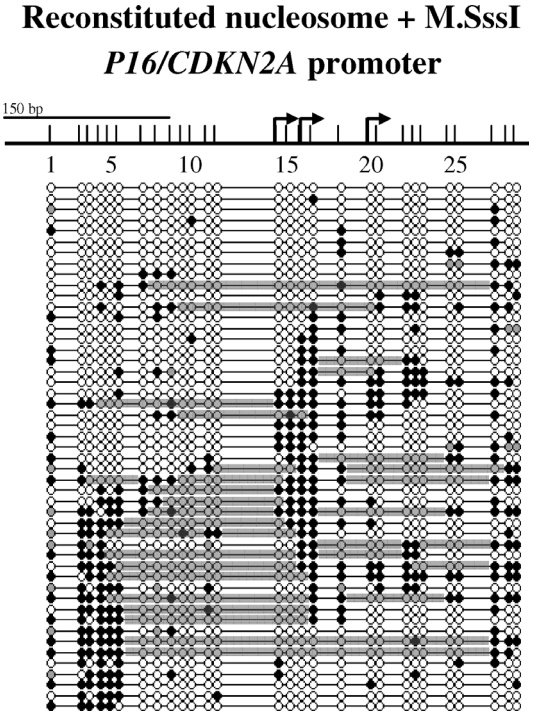

Figure 5. Methylation analysis of *in vitro* reconstituted nucleosomes. Methylation patterns at the *p16* promoter region generated by treating reconstituted nucleosomes with M.SssI for 15 min. Each horizontal line with a string of circles represents the methylation profile for one DNA molecule. White circles indicate unmethylated, black circles methylated and grey circle 'undetermined' CpG sites. Bars indicate the inaccessible regions to M.SssI in each individual sequenced molecule using the 2:2 patch definition (see Figures 6 and 7).

in the reconstituted nucleosomes, which were not present when purified DNA was used as the substrate, suggests that this method has applicability toward studying native chromatin structures.

Accessibility of native chromatin to M.SssI

We prepared nuclei from LD419 and J82 cells and analyzed the accessibility of the *p16* promoter regions to M.SssI (Figure 6). Virtually no background methylation was present in this region in either cell type before M.SssI treatment as reported previously (28).

Similar to the result obtained with the reconstituted nucleosomes, clear patches of inaccessibility to M.SssI were present on the promoters from both LD419 and J82 cells, supporting the concept that the method is detecting the positions of individual nucleosomes (Figure 6A and B). In both cell types, completely unmethylated or scarcely methylated molecules were observed. This might reflect a fraction of the promoters which may exist in a less accessible configuration such as the 30 nm fiber, or the inability of the methylase to access the chromatin due to technical limitations.

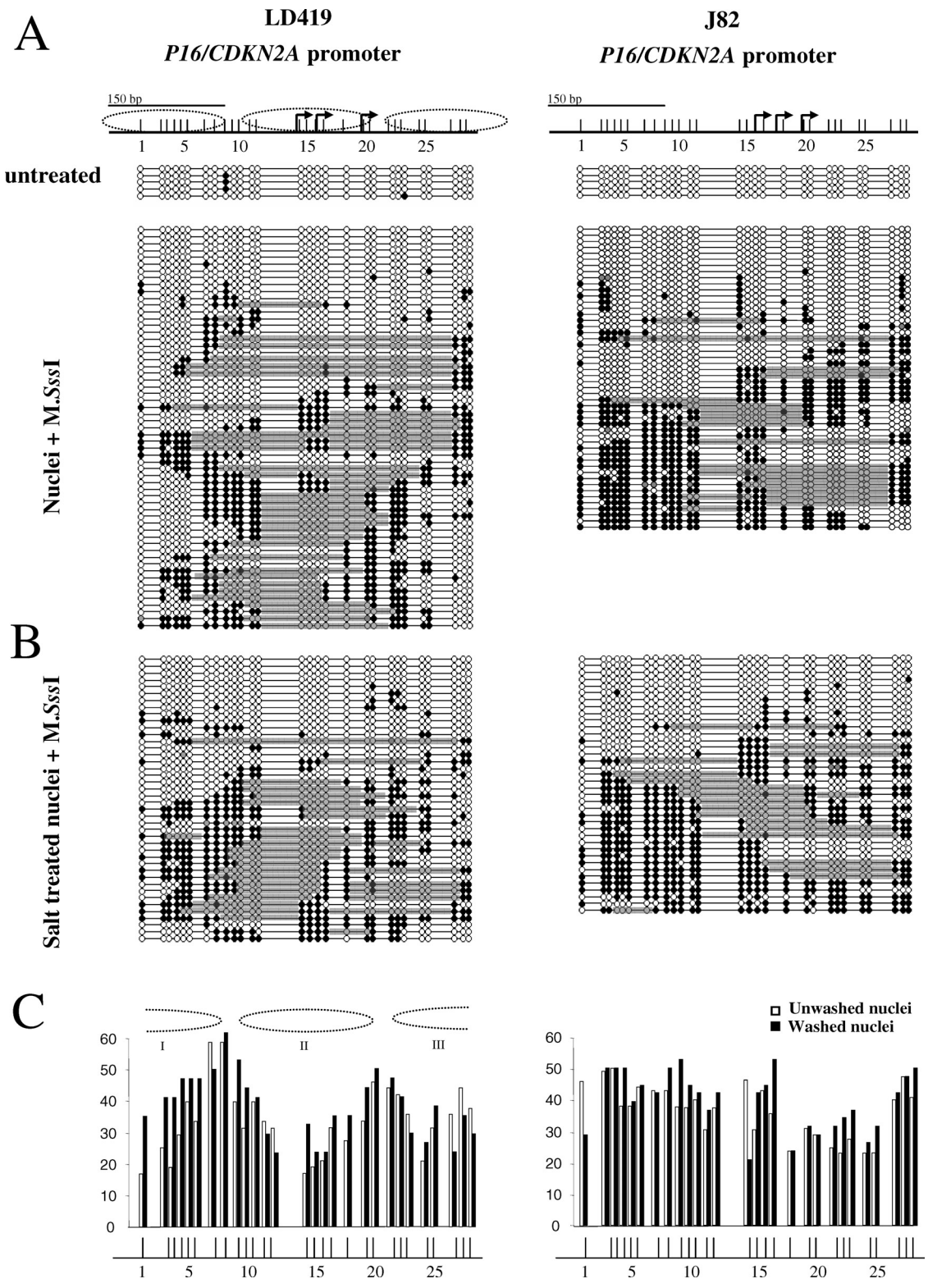

Figure 6. Accessibility of native chromatin to M.SssI at the *p16* promoter region. Left panel: nuclei extracted from low *p16* expressing LD419 cells. Right panel: nuclei extracted from high *p16* expressing J82 cells. (**A**) Nuclei treated with M.SssI for 15 min. (**B**) Nuclei pre-washed with 0.4 M NaCl were treated with M.SssI for 15 min. Each horizontal line with a string of circles represents the methylation profile for a single p16 promoter molecule. Open circles, unmethylated CpG sites, closed circles, methylated CpG sites. For all sequences, the gray bars indicate nucleosomal patches defined as at least two consecutively unmethylated sites flanked on each side by at least two consecutively methylated CpG sites (**C**) Methylation status of individual CpG sites for nuclear and salt washed nuclear preparations. The dotted ovals on the map on the top of the figure show the positions of inaccessible regions to M.SssI based on methylation status at individual CpG sites.

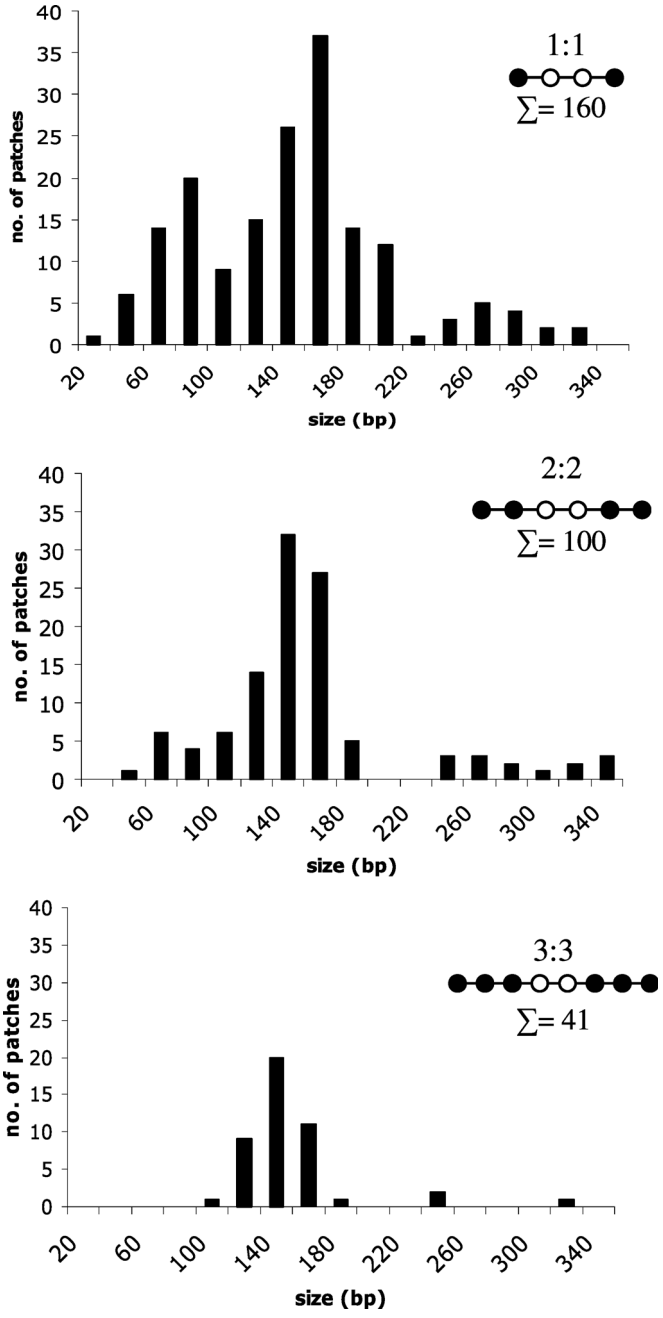

Figure 7. Distribution of patch sizes using three definitions for a patch. These were defined as at least two consecutively unmethylated sites flanked on each side by 1, 2 or 3 consecutively methylated CpG sites (1:1, 2:2 or 3:3 definition, respectively). For the 2:2 and 3:3 definitions, the occurrence of one methylated site did not break the contiguity of a patch. The sum of total patches found for both washed and unwashed nuclei data, using each definition, is indicated on the upper right side of the graphs.

For determination of nucleosome positions, we compared three definitions of a nucleosomal patch. These were defined as at least two consecutively unmethylated sites flanked by 1, 2 or 3 consecutively methylated CpG sites on both sides (Figure 7). All three definitions gave a maximum peak at 120–180 bp corresponding to the expected size of a nucleosome. However, using the 1–1 definition, another peak at the 60–80 bp was observed. This may reflect stochastic methylation by M.SssI, or occasional accessibility of some CpG sites within the core particles, as shown by others (18,19). Both the 2–2 and 3–3 definitions reduced the number of small-sized patches. However, the 3–3 definition was very stringent and resulted in loss of positive data (41 compared with 100 patches). Therefore, the 2–2 definition was further used for analyses of nucleosomal positioning.

Interestingly, the analysis of single promoter sequences showed a clear difference in the positioning and possibly in the number of nucleosomes that could be seen in the two cell types (Figure 6). In LD419 nuclei, many individual promoters had one nucleosome clearly positioned and additional two inaccessible regions spanning the two ends of the analyzed region, suggesting the presence of more nucleosomes. Regions of accessibility were limited to small areas of ~50–70 bp most probably correlating with linker DNA. In contrast, most promoter molecules in the highly *p16* expressing J82 cells contained only one nucleosome. The areas accessible to M.SssI were larger in these cells compared with LD419 fibroblasts. Specifically, the region upstream of the TISs was highly accessible in 45% of the promoters in these cells, indicating the lack of positioned nucleosomes correlating with the high levels of transcription from this promoter. Pre-wash of the nuclei with 0.4 M NaCl before M.SssI treatment, which removes most non-nucleosomal proteins from chromatin (22), caused a small reduction in size of the protected patches (Figure 6B). However, it did not markedly alter their number and overall organization, thus validating that these are indeed nucleosomes. Interestingly, while the translational nucleosome positioning in LD419 seemed to vary only to a minor extent, the nucleosomes in J82 cells were much more heterogeneously positioned, possibly reflecting the dynamics of a more active promoter. Thus, this method allowed us to see that in both cell types, each promoter had a unique arrangement of nucleosomes showing that their 'positioning' is not absolute. When the percentage of methylation was calculated for each CpG site in both washed and unwashed nuclei (Figure 6C), the overall pattern of protection recapitulated the chromatin organization mapped by the MNase assay (compare with Figure 2), correlating to nucleosomes I, II and III, in LD419 cells and to the hypersensitive region in J82 cells. Thus, averaging of the results derived from our method detects similar results obtained by the commonly used methods. However, its single molecule resolution enables one to see the dynamic nature of the promoter.

DISCUSSION

Many detailed studies on the roles of chromatin structure in transcriptional regulation have compared active and inactive promoters in simple eukaryotic organisms, such as yeast (16,17,31). However, the mechanisms by which endogenous human CpG island promoters in mammalian cells are regulated is less well understood (32,33). This paucity of information led us to study the composition of the CpG island promoters of *p16*/*CDKN2A*.

Conventional approaches are not sensitive enough to discern the organization of individual promoter molecules. While high resolution techniques involving primer extension

showed multiple nucleosome translational frames (4) as was found in the present work, these still rely on nuclease digestion. By definition, this means that a promoter could not be studied as a single intact entity until now. The method presented here to footprint DNA–protein interactions at single DNA molecule resolution relies on the known resistance of nucleosomal DNA to M.SssI modification (18,19) coupled with the exquisite sensitivity afforded by the cloning and sequencing of individual progeny molecules.

Several lines of evidence suggest that the 120–180 bp inaccessible patches we observed in the *p16/CDKN2A* promoter correspond to the presence of nucleosomes. First, their mean size reflects the expected size of a core nucleosome. These patches were also present on nucleosomes reconstituted using purified histones. The differences in patch sizes may be attributed to varying degrees of accessibility of M.SssI to the DNA as it approaches the nucleosomal pseudodyad (18,19). Second, the average patch positions correspond to the patterns detected by traditional MNase digestion. Finally, pre-washing with 0.4 M salt, which is known to remove most non-histone binding proteins, did not markedly alter the patch distribution. However, regions upstream of the TISs became slightly more accessible to M.SssI, especially in high p16 expressing J82 cells (Figure 6C), indicating that DNA binding proteins may also restrict M.SssI accessibility (34,35). In some of the promoters in which we find patches which are significantly larger than 120–170 bp, we believe these to reflect compaction of nucleosomes in a way which did not enable M.SssI access to the linker DNA. Thus, we conclude that the patches correlate with the approximate positions of nucleosomes on single molecules. This new approach substantially increases the resolution of analysis of protein–DNA interactions. It is limited by the fact that it relies on the density of CpG sites found in the area analyzed and that only sites unmethylated before M.SssI treatment can be analyzed. However, while the mammalian genome is generally CpG repressed (36), ~40% of mammalian genes have promoters and exonic regions containing CpG islands (37), which are normally unmethylated (38), meaning that they can be analyzed by this approach. Since organisms such as *Saccharomyces cerevisiae* and *Drosophila melanogaster* are not CpG depleted (36), this method should allow for a high resolution analysis of nucleosomal positioning in these species. Another limitation is that while the outer limits of patch size can be determined, the exact sizes cannot. This problem may be overcome in the future by combining CpG-specific (M.SssI) and GpC-specific methyltransferases (M.CviPI) (39), to increase the density of methylated sites.

Application of this method, which reflects the state of a single promoter molecule 'frozen' in time, revealed different dynamics of the promoters of two cell types with markedly different levels of *p16* gene expression. Many of the promoters in the low expressing LD419 cells had nucleosomes organized in a quite conserved pattern which correlated to nucleosomes I, II and III mapped by the MNase assay. However, in the highly expressing J82 cells only one or two nucleosomes were detected, which were more dynamically organized. Since nucleosomes are often moved or disassembled (13) to allow the transcriptional machinery access (3,5,8,31,40) this could reflect nucleosomal remodeling which may enable the increased level of *p16* expression.

Apart from analyzing nucleosome positioning this method may be useful to detect footprints of regulatory proteins acting on various promoters. Furthermore, the combination of cross linking prior to treatment with M.SssI might provide an even higher detailed profile of the promoters analyzed (E. Nili Gal-Yam, S. Jeong, P.A. Jones, unpublished data).

In summary, we have modified a technique by Kladde and Simpson (18) to analyze promoters at single molecule resolution. The method does not rely on cutting with nucleases, so that the relevant nucleosomes and transcription factor footprints are maintained on the replica DNA molecules allowing us to see how the promoter functions as a unit. This approach provides a powerful tool to investigate dynamic changes involved in nucleosome remodeling and transcriptional activation.

ACKNOWLEDGEMENTS

The authors thank Drs Judd Rice, Woojin An and Deborah L. Johnson for critical comments on the manuscript, S. Ramu for helping with genomic bisulfite sequencing. This project was supported by the National Institute of Health grant CA 82422 and 83867 and the Max Kade foundation (to G.E.). Funding to pay the Open Access publication charges for this article was provided by NIH Grant CA 83867 and CA 82422.

Conflict of interest statement. None declared.

REFERENCES

1. Soutoglou,E. and Talianidis,I. (2002) Coordination of PIC assembly and chromatin remodeling during differentiation-induced gene activation. *Science*, **295**, 1901–1904.
2. Metivier,R., Penot,G., Hubner,M.R., Reid,G., Brand,H., Kos,M. and Gannon,F. (2003) Estrogen receptor-alpha directs ordered, cyclical, and combinatorial recruitment of cofactors on a natural target promoter. *Cell*, **115**, 751–763.
3. Clark,D.J. and Felsenfeld,G. (1992) A nucleosome core is transferred out of the path of a transcribing polymerase. *Cell*, **71**, 11–22.
4. Fragoso,G., John,S., Roberts,M.S. and Hager,G.L. (1995) Nucleosome positioning on the MMTV LTR results from the frequency-biased occupancy of multiple frames. *Genes Dev*, **9**, 1933–1947.
5. Lorch,Y., LaPointe,J.W. and Kornberg,R.D. (1987) Nucleosomes inhibit the initiation of transcription but allow chain elongation with the displacement of histones. *Cell*, **49**, 203–210.
6. Studitsky,V.M., Clark,D.J. and Felsenfeld,G. (1994) A histone octamer can step around a transcribing polymerase without leaving the template. *Cell*, **76**, 371–382.
7. Studitsky,V.M., Clark,D.J. and Felsenfeld,G. (1995) Overcoming a nucleosomal barrier to transcription. *Cell*, **83**, 19–27.
8. Workman,J.L. and Kingston,R.E. (1998) Alteration of nucleosome structure as a mechanism of transcriptional regulation. *Annu. Rev. Biochem.*, **67**, 545–579.
9. Rice,J.C. and Allis,C.D. (2001) Histone methylation versus histone acetylation: new insights into epigenetic regulation. *Curr. Opin. Cell Biol.*, **13**, 263–273.
10. Lachner,M., O'Sullivan,R.J. and Jenuwein,T. (2003) An epigenetic road map for histone lysine methylation. *J. Cell Sci.*, **116**, 2117–2124.
11. Tsukiyama,T., Becker,P.B. and Wu,C. (1994) ATP-dependent nucleosome disruption at a heat-shock promoter mediated by binding of GAGA transcription factor. *Nature*, **367**, 525–532.
12. Boeger,H., Griesenbeck,J., Strattan,J.S. and Kornberg,R.D. (2003) Nucleosomes unfold completely at a transcriptionally active promoter. *Mol. Cell*, **11**, 1587–1598.
13. Boeger,H., Griesenbeck,J., Strattan,J.S. and Kornberg,R.D. (2004) Removal of promoter nucleosomes by disassembly rather than sliding in vivo. *Mol. Cell*, **14**, 667–673.

14. Lusser,A. and Kadonaga,J.T. (2003) Chromatin remodeling by ATP-dependent molecular machines. *Bioessays*, **25**, 1192–1200.
15. Studitsky,V.M., Walter,W., Kireeva,M., Kashlev,M. and Felsenfeld,G. (2004) Chromatin remodeling by RNA polymerases. *Trends Biochem. Sci*., **29**, 127–135.
16. Thoma,F. (1996) Mapping of nucleosome positions. *Methods Enzymol*., **274**, 197–214.
17. Elgin,C.R. and Workman,J.L. (2000) *Chromatin Structure and Gene Expression*. Oxford University Press, Oxford, UK.
18. Kladde,M.P. and Simpson,R.T. (1996) Chromatin structure mapping in vivo using methyltransferases. *Methods Enzymol*., **274**, 214–233.
19. Okuwaki,M. and Verreault,A. (2004) Maintenance DNA methylation of nucleosome core particles. *J. Biol. Chem*., **279**, 2904–2912.
20. Nguyen,C.T., Gonzales,F.A. and Jones,P.A. (2001) Altered chromatin structure associated with methylation-induced gene silencing in cancer cells: correlation of accessibility, methylation, MeCP2 binding and acetylation. *Nucleic Acids Res*., **29**, 4598–4606.
21. Cheng,J.C., Weisenberger,D.J., Gonzales,F.A., Liang,G., Xu,G.L., Hu,Y.G., Marquez,V.E. and Jones,P.A. (2004) Continuous zebularine treatment effectively sustains demethylation in human bladder cancer cells. *Mol. Cell. Biol*., **24**, 1270–1278.
22. Ausubel,F.M., Brent,R., Kingston,R.E., Moore,D.D., Seidman,J.G., Smith,J.A. and Struhl,K. (2002) *Chromatin Assembly and Analysis. Current Protocols of Molecular Biology*. Chapter 21, Unit 21.5. John Wiley & Sons, Inc, IN.
23. Stein,A. (1989) Reconstitution of chromatin from purified components. *Methods Enzymol*., **170**, 585–603.
24. Gonzalgo,M.L., Hayashida,T., Bender,C.M., Pao,M.M., Tsai,Y.C., Gonzales,F.A., Nguyen,H.D., Nguyen,T.T. and Jones,P.A. (1998) The role of DNA methylation in expression of the *p19/p16* locus in human bladder cancer cell lines. *Cancer Res*., **58**, 1245–1252.
25. Hayes,J.J. and Lee,K.M. (1997) *In vitro* reconstitution and analysis of mononucleosomes containing defined DNAs and proteins. *Methods*, **12**, 2–9.
26. Frommer,M., McDonald,L.E., Millar,D.S., Collis,C.M., Watt,F., Grigg,G.W., Molloy,P.L. and Paul,C.L. (1992) A genomic sequencing protocol that yields a positive display of 5-methylcytosine residues in individual DNA strands. *Proc. Natl Acad. Sci. USA*, **89**, 1827–1831.
27. Pao,M.M., Tsutsumi,M., Liang,G., Uzvolgyi,E., Gonzales,F.A. and Jones,P.A. (2001) The endothelin receptor B (EDNRB) promoter displays heterogeneous, site specific methylation patterns in normal and tumor cells. *Hum. Mol. Genet*., **10**, 903–910.
28. Nguyen,C.T., Weisenberger,D.J., Velicescu,M., Gonzales,F.A., Lin,J.C., Liang,G. and Jones,P.A. (2002) Histone H3-lysine 9 methylation is associated with aberrant gene silencing in cancer cells and is rapidly reversed by 5-aza-2′-deoxycytidine. *Cancer Res*., **62**, 6456–6461.
29. Hara,E., Smith,R., Parry,D., Tahara,H., Stone,S. and Peters,G. (1996) Regulation of p16CDKN2 expression and its implications for cell immortalization and senescence. *Mol. Cell. Biol*., **16**, 859–867.
30. Ura,K., Hayes,J.J. and Wolffe,A.P. (1995) A positive role for nucleosome mobility in the transcriptional activity of chromatin templates: restriction by linker histones. *EMBO J*., **14**, 3752–3765.
31. Mellor,J. and Morillon,A. (2004) ISWI complexes in *Saccharomyces cer*evisiae. *Biochim. Biophys. Acta*, **1677**, 100–112.
32. Wolf,S.F. and Migeon,B.R. (1985) Clusters of CpG dinucleotides implicated by nuclease hypersensitivity as control elements of housekeeping genes. *Nature*, **314**, 467–469.
33. Patel,S.A., Graunke,D.M. and Pieper,R.O. (1997) Aberrant silencing of the CpG island-containing human O6-methylguanine DNA methyltransferase gene is associated with the loss of nucleosome-like positioning. *Mol. Cell. Biol*., **17**, 5813–5822.
34. Kochanek,S., Renz,D. and Doerfler,W. (1993) Probing DNA–protein interactions in vitro with the CpG DNA methyltransferase. *Nucleic Acids Res*., **21**, 2339–2342.
35. Macleod,D., Charlton,J., Mullins,J. and Bird,A.P. (1994) Sp1 sites in the mouse aprt gene promoter are required to prevent methylation of the CpG island. *Genes Dev*., **8**, 2282–2292.
36. Takai,D. and Jones,P.A. (2002) Comprehensive analysis of CpG islands in human chromosomes 21 and 22. *Proc. Natl Acad. Sci. USA*, **99**, 3740–3745.
37. Larsen,F., Gundersen,G., Lopez,R. and Prydz,H. (1992) CpG islands as gene markers in the human genome. *Genomics*, **13**, 1095–1107.
38. Cross,S.H. and Bird,A.P. (1995) CpG islands and genes. *Curr. Opin. Genet. Dev*., **5**, 309–314.
39. Jessen,W.J., Dhasarathy,A., Hoose,S.A., Carvin,C.D., Risinger,A.L. and Kladde,M.P. (2004) Mapping chromatin structure *in vivo* using DNA methyltransferases. *Methods*, **33**, 68–80.
40. Han,M. and Grunstein,M. (1988) Nucleosome loss activates yeast downstream promoters in vivo. *Cell*, **55**, 1137–1145.